Fracture Toughness Evaluation for magnetostrictive problem using COMSOL-Multiphysics

Awani Bhushan[*1], S.K. Panda[1].
[1]Indian Institute of Technology (BHU) Varanasi
*Corresponding author: Department of Mechanical Engineering, IIT (BHU) Varanasi, awanibhu@gmail.com

Abstract: Even though failure due to presence of flaws, inclusions, cracks or crack like defects has been observed in structural components operated under magnetic fields. The creation of the ferrous man-made structures, however, the formulations of various fracture theories and the understanding of this phenomenon rapidly accelerated during the 20th century. It should be understood clearly that catastrophic consequences of structural failure is sometimes hard to avoid because the factors involved in predicting fracture are very complex. In this manuscript, the influence of magnetostriction on fracture behaviour of ferri or ferromagnetic materials has been studied with the help of energy release rate of cracked specimens subjected under electro-magnetic environment. The derived contour integral has been used to compute the path independent integral using comsol-multiphysics [1]. The fracture toughness (KIc) has been estimated with the help of already evaluated path independent integral using appropriate ASTM standards. Magnetization model (anhysteretic) has been assumed for the magnetostrictive material, which is specified using the Langevin function. The influence of magnetic field on fracture toughness parameters has been significant. The fracture toughness parameter has been saturated at saturated magnetization.

Keywords: Universal 3D *J*-integral, Fracture toughness, magneto-thermo-elasticity, Magnetostriction, Thermo-mechanical

1. Introduction

Materials with large magnetostriction are broadly used in sensors, actuators, energy-harvesters, and micro electro-mechanical systems[2–4]. Magnetostriction of ferromagnetic materials describes the change of their shape or dimension in response to the reorientation of magnetization under the influence of externally applied magnetic field. Magnetic shape memory materials are likely to have a high potential in the design of a different kind of actuating devices and sensors [5–8]. The presence of crack in these materials in a magnetostrictive environment has been a great challenge for many scientists and engineers to characterize the crack parameter. It is required to formulate the crack parameter like stress-intensity factor or J-integral to compute numerically and further experimental validation. One of the approach is introduced by Rice[9] for two dimensional field and further extended to three dimensional thermo-elastic, inertial field by Kishimoto et. al[10]. The numerical computation of three dimensional cracked problem has been studied by [11,12] for bimodular field and thermally induced stresses in the near-wellbore region during invasion of mud by Wang et. al[13]. The three dimensional path independent integral has been derived for magnetic field with multiple loading has been Bhushan et al[1].

This manuscript deals with formulation of path independent magnetostrictive 3D integral for magneto-elastic environment. The stress-intensity factor has been formulated from path independent integral. The path-independence of the derived integral has been proved from numerical computation using FE software package (COMSOL-multiphysics). The stress intensity factor has calculated from path independent integral.

2. Formulation of Integral

The formulation of path independent integral is similar energy conservation concept as followed in [1]. The integral is focused only for magnetostrictive problem. Further stress intensity factor has been derived from integral. The derivation of three dimensional path independent integral has been started with the schematic diagram of a plate containing a crack as shown Fig. 1. In which, the crack tip is assumed to virtually move an infinitesimally small distance from the fixed frame at O to moving frame at O_1. The direction of X_2 and

x_2 are perpendicular to the crack surface corresponding to *O* and O_1 respectively. Two contour paths are chosen, the first one being the outer contour noted by path Γ_1 curves and the second contour Γ_2 can be any arbitrary contour surrounding the crack surfaces. The region enclosed by these two contours is A_1 and the area bounded by the crack plane and the second contour is A_2. Now stating the equilibrium equations for a stressed continuum of volume *V* subjected to arbitrary traction T and body forces *F*:

$$\sigma_{ij,j} + F_i = \rho \ddot{u}_i \tag{1}$$

Where, σ_{ij}, F_i, ρ and u_i are stress-tensor, body force per unit volume, density of solid and displacement respectively where the first and second dots specify the first or second time derivative of displacement. Multiplying $\dot{u}_i$ on both sides of Eq. (1) and integrating over the body volume *V*

$$\iiint_V (\sigma_{ij,j} + F_i)\dot{u}_i \; dV = \iiint_V \rho \ddot{u}_i \dot{u}_i \, dV \tag{2}$$

Now expanding $(\sigma_{ij}\,\dot{u}_i)_{,j} = \sigma_{ij,j}\dot{u}_i + \sigma_{ij}\,\dot{u}_{i,j}$, the first part of the integral of Eq. (2) after rearrangement

$$\iiint_V \sigma_{ij,j}\,\dot{u}_i \, dV = \iiint_V (\sigma_{ij}\,\dot{u}_i)_{,j} \, dV - \iiint_V \sigma_{ij}\,\dot{u}_{i,j} \, dV \tag{3}$$

Now traction on a small differential element on the contour surface can be expressed as

$$T_i = \sigma_{ij}\, n_j \tag{4}$$

where, n_j is the outward normal vector.

Substituting traction form into the integral equations formulated above and using Gauss's Theorem (divergence theorem), it can be written as

$$\iiint_V (\sigma_{ij}\dot{u}_i)_{,j} \; dV = \iint_S \sigma_{ij}\,\dot{u}_i\, n_j \; dS = \iint_S T_i\,\dot{u}_i \, dS \tag{5}$$

Introducing Eq. (5) into Eq. (3) and using strain derivatives $\dot{\in}_{ij}$ for displacement derivative, it is shown that

$$\iiint_V (\sigma_{ij,j}\,\dot{u}_i) \; dV = \iint_S T_i\,\dot{u}_i \, dS - \iiint_V \sigma_{ij}\dot{\varepsilon}_{ij} \, dV \tag{6}$$

Now, Eq. (2) can be written as

$$\iint_S T_i \dot{u}_i dS + \iiint_V F_i \dot{u}_i \, dV = \iiint_V \rho \ddot{u}_i u_i \; dV + \iiint_V \sigma_{ij}\dot{\varepsilon}_{ij} \; dV \tag{7}$$

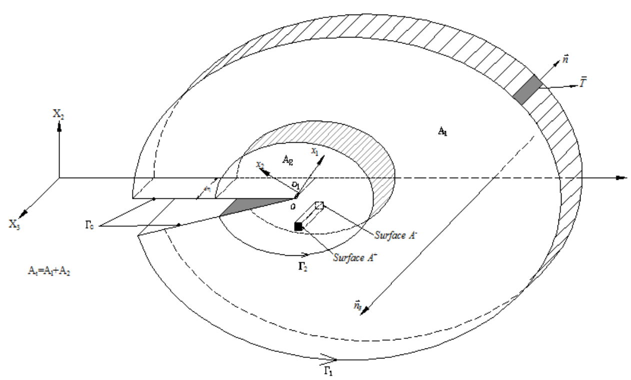

Fig. 1. Configuration of crack tip {Γ_1 (arbitrary curve surrounding area A_1), Γ_c (curve along the crack surface), A_2 (fracture process region), Γ_2 (boundary of A_2)} around a region of infinitesimal thickness enclosing the Crack Front.

For an infinitesimal virtual crack extension, the energy release rate can be evaluated from Eq. (7) for a differential change *dl* of the propagating crack as similar to time derivatives. This is expressed as

$$\int_{\Gamma_1+\Gamma_c} T_i \frac{du_i}{dl} d\Gamma + \iint_{A_1} F_i \frac{du_i}{dl} dA = \iint_{A_1} \rho \ddot{u}_i \frac{du_i}{dl} dA + \iint_{A_1} \sigma_{ij} \frac{d\varepsilon_{ij}}{dl} dA + J^u \tag{8}$$

where, J^u is the rate of change of energy of material in the fracture process region for name say a generalized universal integral, be it unimodular or bimodular. We can introduce zero integral terms with reference to contour Γ_2 with an integral evaluated along the contour path and opposite the contour path by adding and subtracting the term $\int_{\Gamma_2} T_i \frac{du_i}{dl} d\Gamma$ to Eq. (8) as

$$\int_{\Gamma_2} T_i \frac{du_i}{dl} d\Gamma + \int_{-\Gamma_2} T_i \frac{du_i}{dl} d\Gamma + \iint_{A_1} F_i \frac{du_i}{dl} dA = \iint_{A_1} \rho \ddot{u}_i \frac{du_i}{dl} dA + \iint_{A_1} \sigma_{ij} \frac{d\varepsilon_{ij}}{dl} dA + J^u - \int_{\Gamma_1+\Gamma_c} T_i \frac{du_i}{dl} d\Gamma \tag{9}$$

Upon rearrangement following expressions for energy release rate J^u is obtained.

$$J^u = \int_{\Gamma_1+\Gamma_c-\Gamma_2} T_i \frac{du_i}{dl} d\Gamma + \int_{\Gamma_2} T_i \frac{du_i}{dl} + \iint_{A_1} \left[(F_i - \rho \ddot{u}_i) \frac{du_i}{dl} - \left(\sigma_{ij} \frac{d\varepsilon_{ij}}{dl} \right) \right] dA \tag{10}$$

$$J^u = \iint_{A_1} (\sigma_{ij} \frac{du_i}{dl})_{,j}\, dA + \int_{\Gamma_2} T_i \frac{du_i}{dl} d\Gamma + \iint_{A_1} [(F_i - \rho \ddot{u}_i) \frac{du_i}{dl} - (\sigma_{ij} \frac{d\varepsilon_{ij}}{dl})] dA \tag{11}$$

$$J^u = \iint_{A_1} [(\sigma_{ij} \frac{du_i}{dl})_{,j} + (F_i - \rho \ddot{u}_i) \frac{du_i}{dl} - \sigma_{ij} \frac{d\varepsilon_{ij}}{dl}]\, dA + \int_{\Gamma_2} T_i \frac{du_i}{dl} d\Gamma \tag{12}$$

Using Eq. (1), the first term of area integral in Eq. (12) vanishes and the integral may be written as

$$J^u = \int_{\Gamma_2} T_i \frac{du_i}{dl} d\Gamma \tag{13}$$

With reference to Fig. 2, transformation equations from the fixed frame $O - X_1, X_2$ to moving frame $O_1 - x_1, x_2$ for the infinitesimal crack extension can be expressed as

$$\begin{aligned} x_1 &= X_1 \cos\theta_0 + X_2 \sin\theta_0 - l \\ x_2 &= - X_1 \sin\theta_0 + X_2 \cos\theta_0 \end{aligned} \tag{14}$$

$$\begin{aligned} X_1 &= x_1 \cos\theta_0 - x_2 \cos\theta_0 + l \cos\theta_0 \\ X_2 &= x_1 \sin\theta_0 + x_2 \cos\theta_0 + l \sin\theta_0 \end{aligned} \tag{15}$$

Similarly, displacements for the fixed frame $O - X_1, X_2$ is given by

$$\begin{aligned} u_i(X_1, X_2, l) = u_i(&x_1 \cos\theta_0 + x_2 \sin\theta_0 \\ &- l, - x_1 \sin\theta_0 + x_2 \cos\theta_0, l) \end{aligned} \tag{16}$$

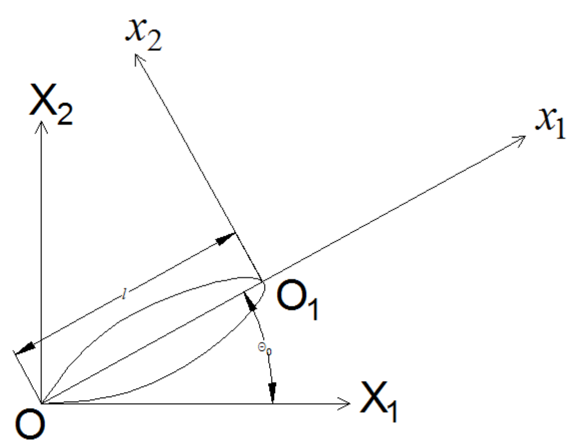

(a)

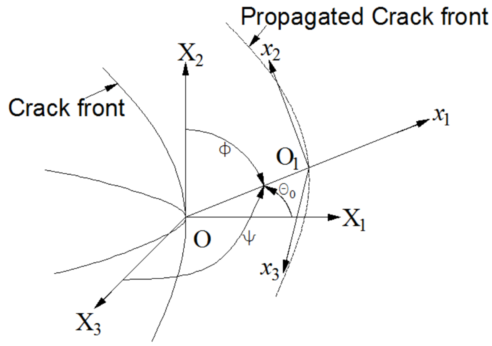

(b)

Fig. 2. Representation of propagation of crack tip from O to O_1 in (a) 2D boundary and (b) 3D domain

$$\frac{du_i}{dl}=\frac{\partial u_i}{\partial l}+\frac{\partial u_i}{\partial x_i}\frac{\partial x_i}{\partial l}=\frac{\partial u_i}{\partial l}+\frac{\partial u_i}{\partial x_1}\frac{\partial x_1}{\delta l}+\frac{\partial u_i}{\partial x_2}\frac{\partial x_2}{\partial l} \tag{17}$$

$$\frac{\partial u_i}{\partial x_1}\frac{\partial x_1}{\partial l}=-\frac{\partial u_i}{\partial x_1}\ ;\ \frac{\partial x_2}{\partial l}=0 \tag{18}$$

$$\frac{du_i}{dl}=\frac{\partial u_i}{\partial l}-\frac{\partial u_i}{\partial x_1} \tag{19}$$

Now substitution of Eq. (19) into Eq. (13) gives,

$$J^u=\int_{\Gamma_2} T_i\left(\frac{\partial u_i}{\partial l}-\frac{\partial u_i}{\partial x_1}\right)d\Gamma \tag{20}$$

Here, J^u*-integral* is the crack driving force or also known as the energy release rate during crack extension.

We assume that the fracture process region does not depend upon load conditions or upon geometry of body or crack. Hence, the process region is assumed to be constant in dimensions and moving along with the same speed as the crack tip, and hence, $\frac{\partial u_i}{\partial l}=0$ holds in Γ_2.

Then, Eq. (20) is simplify to

$$J^u=-\int_{\Gamma_2} T_i\left(\frac{\partial u_i}{\partial x_1}\right)d\Gamma \tag{21}$$

We obtain from Eq. (14), (15) & (16)

$$\frac{\partial u_i}{\partial x_1}=\cos\theta_0\frac{\partial u_i}{\partial X_1}+\sin\theta_0\frac{\partial u_i}{\partial X_2} \tag{22}$$

Substituting Eq. (22) in Eq. (21) the integral equation becomes

$$J^u=-\int_{\Gamma_2} T_i\left(\cos\theta_0\frac{\partial u_i}{\partial X_1}+\sin\theta_0\frac{\partial u_i}{\partial X_2}\right)d\Gamma \tag{23}$$

For any arbitrary orientation θ_0 of the propagating crack front, the J^u can be resolved as

$$J^u=J_1^u\cos\theta_0+J_2^u\sin\theta_0 \tag{24}$$

Taking as single notation J_k^u where k=1, 2 correspond to respective coordinate axes, Eq. (21) can be modified using Eq. (24) as

$$J_k^u=-\int_{\Gamma_2} T_i\frac{\partial u_i}{\partial X_k}d\Gamma \tag{25}$$

However, for verification of that the above integral to be path independent, let us consider another integral surrounding the crack path and expressed as

$$\bar{J}_k^u=-\int_{\Gamma_1+\Gamma_c} T_i\frac{\partial u_i}{\partial X_k}d\Gamma+M_k(A) \tag{26}$$

where, $M_k(A)$ are the terms determined when the area A_1 surrounded by Γ_1,Γ_2 and Γ_c is specified. Now, if both the integral J_k^u and $\bar{J}_k^u$ are different, then we can write

$$\bar{J}_k^u-J_k^u=-\int_{\Gamma_1+\Gamma_c} T_i\frac{\partial u_i}{\partial X_k}d\Gamma+M_k(A)+\int_{\Gamma_2} T_i\frac{\partial u_i}{\partial X_k}d\Gamma \tag{27}$$

$$\bar{J}_k^u-J_k^u=-\int_{\Gamma_1+\Gamma_c-\Gamma_2} T_i\frac{\partial u_i}{\partial X_k}d\Gamma+M_k(A) \tag{28}$$

$$\bar{J}_k^u-J_k^u=-\int_{\Gamma_t} T_i\frac{\partial u_i}{\partial X_k}d\Gamma+M_k(A) \tag{29}$$

$\Gamma_t = \Gamma_1 + \Gamma_c - \Gamma_2$ denotes the contour which surrounds the area A_1.

For path independence $\bar{J}_k^u = J_k^u$ and hence from Eq. (29)

$$M_k(A) = \int_{\Gamma_t} T_i \frac{\partial u_i}{\partial X_k} d\Gamma = \iint_A (\sigma_{ij} \frac{\partial u_i}{\partial X_k})_{,j}\, dA \qquad (30)$$

Therefore,

$$\bar{J}_k^u = J_k^u = \iint_{A_1} (\sigma_{ij} \frac{\partial u_i}{\partial X_k})_{,j}\, dA - \int_{\Gamma_1+\Gamma_c} T_i \frac{\partial u_i}{\partial X_k} d\Gamma \qquad (31)$$

Using Eq. (1), we can write Eq. (31) as

$$J_k^u = \iint_{A_1} \{(\rho \ddot{u}_i - F_i) \frac{\partial u_i}{\partial X_k} + (\sigma_{ij} \frac{\partial \varepsilon_{ij}}{\partial X_k})\} dA - \int_{\Gamma_1+\Gamma_c} T_i \frac{\partial u_i}{\partial X_k} d\Gamma$$

(k=1, 2)

(32)

Now we decompose ε_{ij} as ε_{ij}^e , ε_{ij}^m

$$\varepsilon_{ij} = \varepsilon_{ij}^e + \varepsilon_{ij}^m \qquad (33)$$

where, ε_{ij}^e Elastic Strain Component

ε_{ij}^m Magnetic Strain Component

We take elastic strain energy density function, $W^e\,(\varepsilon_{ij}^e)$ which does not explicitly depend on X_1.

$$\frac{\partial}{\partial \varepsilon_{ij}^e} W^e = \sigma_{ij} \qquad (34)$$

From Magnetostriction Model [14],

$$\lambda\,(t,x) = \sum_{i=0}^{\infty} \gamma_i M^{2i}(t,x) \qquad (35)$$

By assuming or approximating the value of λ to second order,

$$\varepsilon_{ij}^m = \frac{3}{2} \frac{\lambda_s}{M_s^2} M^2(t,x) \qquad (36)$$

where, $\lambda_s \rightarrow$ Saturated Magnetostriction

$M_s \rightarrow$ Saturated Magnetization.

Hence,

$$\varepsilon_{ij} = \varepsilon_{ij}^m + \frac{3}{2} \frac{\lambda_s}{M_s^2} M^2 \qquad (37)$$

As,

$$J_k^u = \iint_{A_1} (\rho \ddot{u}_i - F_i) \frac{\partial u_i}{\partial X_k} dA - \int_{\Gamma_1+\Gamma_c} T_i \frac{\partial u_i}{\partial X_k} d\Gamma + \iint_{A_1} (\sigma_{ij} \frac{\partial \varepsilon_{ij}}{\partial X_k}) dA \qquad (38)$$

Consider,

$$\iint_{A_1} (\sigma_{ij} \frac{\partial \varepsilon_{ij}}{\partial X_k}) dA = \iint_{A_1} \sigma_{ij} (\frac{\partial \varepsilon_{ij}^e}{\partial X_k} + \frac{\partial \varepsilon_{ij}^m}{\partial X_k}) dA \qquad (39)$$

Because of fracture process zone is very small

$$\iint_{A_1} \sigma_{ij} \frac{\partial \varepsilon_{ij}}{\partial X_k} dA = \int_{\Gamma_1+\Gamma_c-\Gamma_2} W^e n_k\, d\Gamma = \int_{\Gamma_1+\Gamma_c} W^e n_k\, d\Gamma \qquad (40)$$

$$\iint_{A_1} \sigma_{ij} \frac{\partial \varepsilon_{ij}^m}{\partial X_k} dA = \iint_{A_1} \sigma_{ij} \frac{3\lambda_s}{M_s^2} \frac{\partial M^2}{\partial X_k} dA \qquad (41)$$

$$\iint_{A_1} \sigma_{ij} \frac{\partial \varepsilon_{ij}^m}{\partial X_k} dA = \iint_{A_1} \sigma_{ij} \frac{3\lambda_s}{M_s^2} M \frac{\partial M}{\partial X_k} dA \qquad (42)$$

We also consider area of fracture process region is diminishing and contour integral [1] $\Gamma_{end} = 0$ Combining all the quantities

$$J_k^u = \int_{\Gamma_1+\Gamma_c} \{W^e n_k - T_i \frac{\partial u_i}{\partial X_k}\} d\Gamma + \iint_{A_1} (\rho \ddot{u}_i - F_i) \frac{\partial u_i}{\partial X_k} dA + \iint_{A_1} \frac{3\lambda_s \sigma_{ij}}{M_s^2} M \frac{\partial M}{\partial X_k} dA \qquad (43)$$

$$J_k^u = (J_k^u)_{2D} \qquad \text{(k = 1, 2)} \qquad (44)$$

Here k will be equal to 1 as we assume crack propagation variation is very small in other directions. And so we can write J_k^u as

$$J_k^u = J_1^u \cos\theta_0 + J_2^u \sin\theta_0 \;\cong\; J_1^u \cos\theta_0 \quad (45)$$

As θ_0 will be very small and so 2nd term will vanish. Hence, k will be equal to 1.

$(J_k^u)_{2D}$ can be taken as constant through the thickness $d\eta$, let $A_t = A_1 + A_2$. And the two faces of this A_t area is $A_t^{\,+}$ and $A_t^{\,-}$. As normal to these two faces are parallel and in opposite directions, the sum of the two area integral is given by the X_3 derivative of the integrand multiplied by $d\eta$. Division of both sides by $d\eta$ gives the pointwise value for the integral and further sum with integrand yields *J* -integral in 3-D.

$$\left(J_k^u\right)_{3D} \Rightarrow (J_k^u)_{2D} + \iint_{A_t} \frac{\partial}{\partial X_3}(J_k^u)_{2D}\, n_3\; dA \quad (46)$$

$$\iint_{A_t} \frac{\partial}{\partial X_3}(J_k^u)_{2D}\, dA = \frac{\partial}{\partial X_3}\iint_{A_t}\{W^e n_k - T_i \frac{\partial u_i}{\partial X_k}\} n_3\; dA + \frac{\partial}{\partial X_3}\iint_{A_t}(\rho\ddot{u}_i - F_i)\frac{\partial u_i}{\partial X_k}\, dA + \iint_{A_t} \frac{3\lambda_s \sigma ij\, M_0}{M_s^{\,2}}\frac{\partial M}{\partial X_k}\; dA \quad (47)$$

All the term except 1st term will vanish in above equation as variation of other terms in the direction n_3 is constant. So, we can write above equation as

$$\iint_{A_t} \frac{\partial}{\partial X_3}(J_k^u)_{2D}\, n_3\; dA = \iint_{A_t} \frac{\partial}{\partial X_3} W^e n_k\, n_3\; dA - \iint_{A_t} \frac{\partial}{\partial X_3}\left(\sigma_{ij}\, n_j \frac{\partial u_i}{\partial X_k}\right) n_3\; dA \quad (48)$$

$$\left(J_k^u\right)_{3D} = \int_{\Gamma_1+\Gamma_c} \{W^e n_k - T_i \frac{\partial u_i}{\partial X_k}\}\, d\Gamma + \iint_{A_t} \frac{\partial}{\partial X_3} W^e n_k\, n_3\; dA - \iint_{A_t} \frac{\partial}{\partial X_3}\left(\sigma_{ij}\, n_j \frac{\partial u_i}{\partial X_k}\right) n_3\; dA + \iint_{A_t}(\rho\ddot{u}_i - F_i)\frac{\partial u_i}{\partial X_k}\, dA + \iint_{A_1} \sigma_{ij}\frac{3\lambda_s}{M_s^{\,2}} M \frac{\partial M}{\partial X_k}\; dA \quad (i, j, k{=}1,2,3) \quad (49)$$

Again,

$$\left(J_k^u\right)_{3D} = J_1^u \cos\theta_0 + J_2^u \cos\Phi + J_3^u \cos\Psi \cong J_1^u \cos\theta_0 \quad (50)$$

After, taking k=1

$$\left(J_k^u\right)_{3D} = \int_{\Gamma_1+\Gamma_c} \{W^e n_1 - T_i \frac{\partial u_i}{\partial X_1}\}\, d\Gamma + \iint_{A_t} \frac{\partial}{\partial X_3} W^e n_1 n_3\; dA + \iint_{A_t}(\rho\ddot{u}_i - F_i)\frac{\partial u_i}{\partial X_1}\, dA - \iint_{A_t} \frac{\partial}{\partial X_3}\left(\sigma_{ij}\, n_j \frac{\partial u_i}{\partial X_1}\right) n_3\; dA + \iint_{A_1} \sigma_{ij}\frac{3\lambda_s}{M_s^{\,2}} M \frac{\partial M}{\partial X_k}\; dA \quad (51)$$

Here, in the above expression, second term will be zero as dot product of normal vector $\left(n_1 \cdot n_3\right)$ is zero and in the third term, *j=1,2* will vanish and only 3 contribute in the expression as follows:

$$\left(J_k^u\right)_{3D} = \int_{\Gamma_1+\Gamma_c} \{W^e n_1 - T_i \frac{\partial u_i}{\partial X_1}\} d\Gamma - \iint_{A_t} (\sigma_{i3} u_{i,3})_{,3}\ dA_1 + \iint_{A_1} (\rho \ddot{u}_i - F_i) \frac{\partial u_i}{\partial X_1} dA_1 + \iint_{A_1} \sigma_{ij} \frac{3\lambda_s}{M_s^2} M \frac{\partial M}{\partial X_k}\ dA$$

$$(i, j = 1,2,3) \qquad (52)$$

In the absence of body forces and material inertia the Eq. (52) can be written as

$$\left(J_k^u\right)_{3D} = \int_{\Gamma_1+\Gamma_c} \{W^e n_1 - T_i \frac{\partial u_i}{\partial X_1}\} d\Gamma - \iint_{A_t} (\sigma_{i3} u_{i,3})_{,3}\ dA_1 + \iint_{A_1} \sigma_{ij} \frac{3\lambda_s}{M_s^2} M \frac{\partial M}{\partial X_k}\ dA$$

$$(i, j = 1,2,3) \qquad (53)$$

Within the elastic limit the fracture toughness K_{Ic} values calculated from critical path independent integral $\left(J_{kc}^u\right)_{3D}$ employing the following expression taken from ASTM E1921-17a [15] and rearranged in following form:

$$K_{Ic} = \sqrt{\frac{\left(J_{kc}^u\right)_{3D} E}{\left(1-\nu^2\right)}} \qquad (54)$$

where, $\left(J_{kc}^u\right)_{3D}$ is the critical path independent integral value which is equivalent to critical energy release rate value for the material having no permissible growth of plastic zone. K_{Ic} is the critical stress intensity factor or fracture toughness. The fracture toughness is the material property estimated with experimental testing. The simulation results may compare with the experimental value for the specific failure load.

3. Finite Element Model Results

Finite element modeling of rectangular cracked bar under the magnetostriction has been developed using COMSOL multiphysics.

Three-dimensional cracked beam geometry has been built and solved under the magnetostrictve environment. The four contours have been taken to prove the path independence of the integral $\left(J_k^u\right)_{3D}$. The integrating contours and magnetic field has been represented in the Fig. 3.

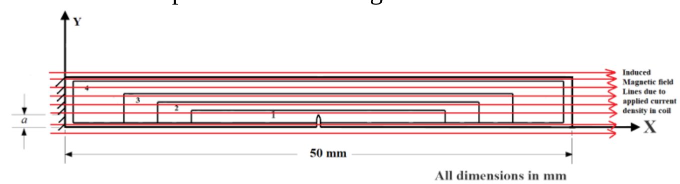

Fig. 3. Integrating contours and applied boundary condition in the magnetic field

The 50 mm cracked beam has been taken with 6mm x 6mm cross-section. The crack length has been taken 1.5 mm. The cracked specimen is surrounded by helical coil which carry the input current to induce magnetostriction over the specimen. The magnetic flux leakage is minimized by the steel housing. Fig.4 illustrate the arrangement of steel housing, helical coil and the cracked specimen.

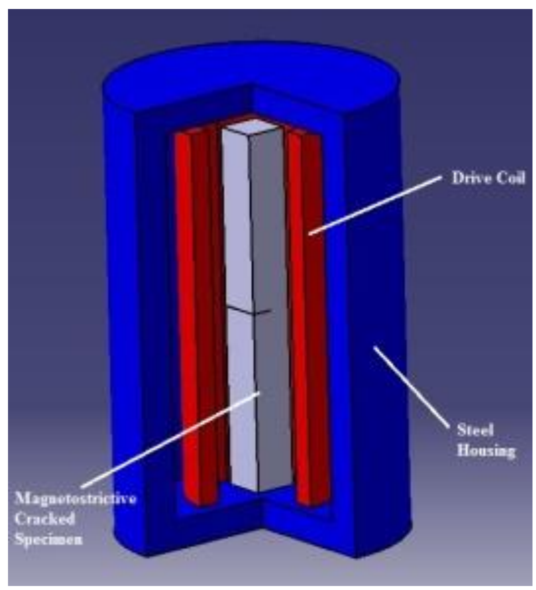

Fig. 4. The arrangement of steel housing, helical coil and the cracked specimen (sectional view)

The magnetization model has been assumed for the magnetostrictive material, which is specified using the Langevin function[14,16,17] as follows:

$$\frac{M}{M_s}=\left[\coth\left(\frac{H_e}{a}\right)-\left(\frac{a}{H_e}\right)\right] \quad (55)$$

where, a is domain density constant with dimensions of magnetic field and H_e is the effective magnetic field.

The material property has been taken for magnetostrictive material is 60 GPa and .3 as modulus of elasticity and Poisson's ratio respectively. Saturated magnetization and saturated magnetostriction are 15×10^5 A/m and 2×10^{-4} respectively and Effective domain density (a) is 7000 A/m.

A mesh convergent model has been taken for the simulations current carrying magnetic field problem. The finite element mesh model contains 92210 tetrahedral elements and 13296 hexahedral elements. The tetrahedral elements are used to mesh steel housing, helical coil, and air domains, whereas the hexahedral elements are used to mesh the cracked specimen as shown in Fig 5.

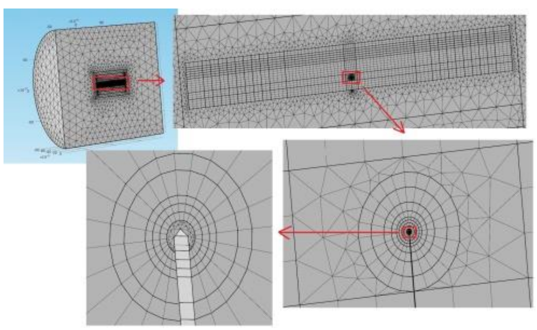

Fig. 5. Mesh distribution of cracked specimen model with steel housing enclosing the drive coil.

The normalized path independent integral has been plotted against the integration contour in the Fig. 6. The path independency of the integral for magnetostrictive problem has been proved for four contours.

Fig. 7 represents the variation of normalized integral $\left(J_k^u\right)_{3D}$ against the increasing current density. The plot shows integral values increased with increasing current density applied on the coil and saturated at the range of 2×10^6 A/m^2. The increase of current density increases the magnetization value over the specimen and saturated at a particular value of current density[18,19]. It is well known that increasing magnetic field increases the magnetization up to saturated magnetization.

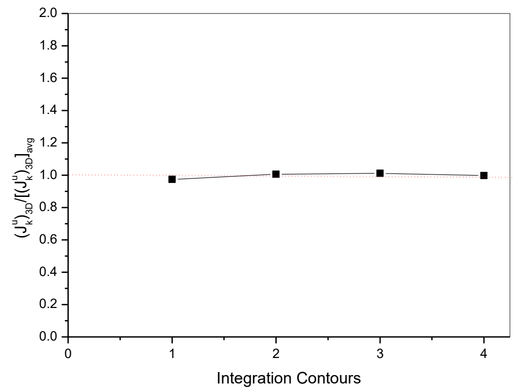

Fig. 6 The integral has been proved for four contours.

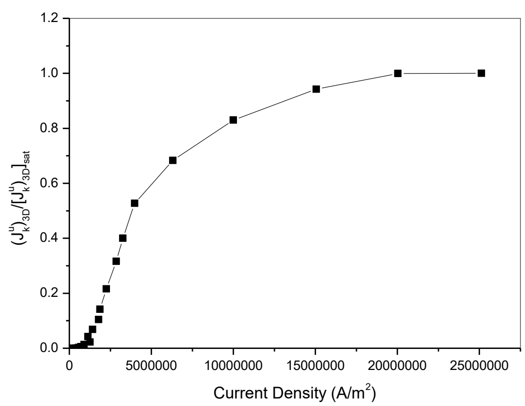

Fig. 7 The variation normalized $\left(J_k^u\right)_{3D}$ integral through increasing current density.

The stress-intensity factor has been evaluated for saturated value of the path independent integral $\left(J_k^u\right)_{3D}$ using Eq. (54). The critical value of stress intensity factor is the fracture toughness.

4. Conclusion

A conservation path independent integral *J* for a straight crack has been proposed to have the physical meaning of energy release rate (both in two dimensional and three dimensional cases) for a homogeneous, isotropic material considering combined effects of magnetostriction. The path independency of the integral $\left(J_k^u\right)_{3D}$ has been proved for four contours. The magnetization saturates after increasing current density. The integral $\left(J_k^u\right)_{3D}$ value saturates at saturated magnetization.

References

[1] Bhushan, A., Panda, S. K., Singh, P. K., Kartheek, P., Kumar, R., and Mittal, Y., 2018, "3D Path Independent Integral for Thermoelastic and Magnetostriction Problem," Mechanics Research Communications.

[2] Wang, H., Zhang, Y. N., Wu, R. Q., Sun, L. Z., Xu, D. S., and Zhang, Z. D., 2013, "Understanding Strong Magnetostriction in Fe 100-XGaxalloys," Scientific Reports, **3**, pp. 1–5.

[3] Clark, A. E., "FerromagneticMaterials, Vol. 1."

[4] Clark, A. E., and Hathaway, K. B., 2000, *Handbook of Giant Magnetostrictive Materials*, Academic, San Diego, 2000.

[5] Handley, R. C. O., Murray, S. J., Marioni, M., Nembach, H., Allen, S. M., Handley, R. C. O., Murray, S. J., Marioni, M., Nembach, H., and Allen, S. M., 2000, "Phenomenology of Giant Magnetic-Field-Induced Strain in Ferromagnetic Shape-Memory Materials (Invited) Phenomenology of Giant Magnetic-Field-Induced Strain in Ferromagnetic Shape-Memory Materials „ Invited …," **4712**.

[6] Murray, S. J., Marioni, M., Allen, S. M., Handley, R. C. O., Lograsso, T. A., Murray, S. J., Marioni, M., Allen, S. M., and Handley, R. C. O., 2000, "6 % Magnetic-Field-Induced Strain by Twin-Boundary Motion in Ferromagnetic Ni – Mn – Ga in Ferromagnetic Ni – Mn – Ga," **886**, pp. 10–13.

[7] Sakon, T., Sasaki, K., Numakura, D., Abe, M., Nojiri, H., Adachi, Y., and Kanomata, T., 2013, "Magnetic Field-Induced Transition in Co-Doped," **54**(1), pp. 9–13.

[8] Sozinov, A., Likhachev, A. A., Lanska, N., and Ullakko, K., 2002, "Giant Magnetic-Field-Induced Strain in NiMnGa Seven-Layered Martensitic Phase," Applied Physics Letters, **80**(10), pp. 1746–1748.

[9] Rice, J. R., 1968, "A Path Independent Integral and the Approximate Analysis of Strain Concentration by Notches and Cracks," Journal of Applied Mechanics, ASME, **35**, pp. 379–386.

[10] Kishimoto, K., Aoki, S., and Sakata, M., 1980, "On the Path Independent Integral-Ĵ," Engineering Fracture Mechanics, **13**(4), pp. 841–850.

[11] Bhushan, A., and Panda, S. K., 2018, "Experimental and Computational Correlation of Fracture Parameters K Ic , J Ic , and G Ic for Unimodular and Bimodular Graphite Components," Journal of Nuclear Materials, **503**, pp. 205–225.

[12] Bhushan, A., Panda, S. K., Singh, S. K., and Khan, D., 2015, "Finite Element Evaluation of J -Integral in 3D for Nuclear Grade Graphite Using COMSOL-Multiphysics," *Proceedings of COMSOL Conference, Pune October 29-30, 2015*, Pune, pp. 1–7.

[13] Wang, Z., and Chen, Y., 2018, "Finite Element Analysis of Thermally Induced Stresses in the Near-Wellbore Region During Invasion of Mud Into Fractures," Journal of Energy Resources Technology, ASME, **140**(May), pp. 1–10.

[14] Dapino, M. J., Smith, R. C., and Flatau, A. B., 2000, "Structural Magnetic Strain Model for Magnetostrictive Transducers," IEEE Transactions on Magnetics, **36**(3), pp. 545–556.

[15] ASTM E1921-17a, 2017, "Standard Test Method for Determination of Reference Temperature , To, for Ferritic Steels in the Transition Range," ASTM Book of Standards, pp. 1–27.

[16] Liorzou, F., Phelps, B., and Atherton, D.

L., 2000, “Macroscopic Models of Magnetization,” IEEE Transactions on Magnetics, **36**(2), pp. 418–428.

[17] Dapino, M. J., Smith, R. C., Faidley, L. E., and Flatau, A. B., 2000, “Coupled Structural-Magnetic Strain and Stress Model for Magnetostrictive Transducers,” Journal of Intelligent Material Systems and Structures, **11**(2), pp. 135–152.

[18] Bhushan, A., Panda, S. K., Mittal, Y., Kartheek, P., and Kumar, R., 2018, “Study of 3D Mathematical Model of Rectangular Bar under Magnetostriction,” *Proceeding of Second International Conference on Mechanical, Automotive and Aerospace Engineering - MAAE 2018*, pp. 14–20.

[19] COMSOL-Multiphysics, T., 2017, *Nonlinear Magnetostrictive Transducer (Tutorial)*.